# EXPERIMENTAL AND THEORETICAL EVALUATION OF A SOLAR CHIMNEY TEST PLANT PART I: THEORETICAL TREATMENT

**Cristiana Brasil Maia**
Departamento de Engenharia Mecânica, Pontifícia Universidade Católica de Minas Gerais – PUC/MG
Av. Dom José Gaspar, 500, Coração Eucarístico, CEP 30535-610, Belo Horizonte, MG, Brasil
cristiana@pucminas.br

**André Guimarães Ferreira**
Curso de Engenharia de Alimentos, DCET, Centro Universitário de Belo Horizonte – UNI-BH
Av. Mário Werneck, 1685, Estoril, CEP 30455-610, Belo Horizonte, MG, Brasil
agferreira@acad.unibh.br

**Ramón Molina Valle**
Departamento de Engenharia Mecânica, Universidade Federal de Minas Gerais – UFMG
Av. Antônio Carlos, 6627, Campus Universitário, CEP 31270-901, Belo Horizonte, MG, Brasil
ramon@demec.ufmg.br

**Márcio Fonte Boa Cortez**
Departamento de Engenharia Mecânica, Universidade Federal de Minas Gerais – UFMG
Av. Antônio Carlos, 6627, Campus Universitário, CEP 31270-901, Belo Horizonte, MG, Brasil
fonteboa@demec.ufmg.br

***Abstract.*** *The solar chimney is a device that uses the incident solar radiation to generate a hot airflow. An experimental and theoretical study was undertaken to evaluate the behavior of the fields of temperature and velocity in the solar chimney. A mathematical model using the Finite Volume Method in Generalized Coordinates was adopted to solve the system of equations which describe the flow. The validation of the proposed mathematical model and the numerical methodology was done through the comparison of the theoretical results and the experimental data obtained in a plant. This paper presents the distribution of the velocity and temperature in the device and the influence of the turbulence model on the characterization of the flow. The result indicated that the developed model can be used as a tool to help on the design of solar chimneys.*

***Keywords****: Solar chimney, Numerical modeling, Solar chimney tests plant*

## 1. Introduction

Nowadays, there is an increasing concerning about the utilization of energy, due to the reduction of the non-conventional sources of energy. Solar energy is a renewable and non pollutant source of energy. The utilization of solar energy can be divided into two major groups: photovoltaic and thermal uses. Some materials can generate electricity from light. Photovoltaic applications use this property to generate solar power. Thermal applications use the solar energy to heat water, to produce electrical energy and to dry agricultural products.

The concept of the solar chimney was originally developed by Professor J. Schlaich. A typical solar chimney consists on a tower, a solar collector, which is composed by a translucent cover and by the ground and a turbine with a generator (Fig. 1). A portion of the incident solar radiation is transmitted by the cover and reaches the ground. The solar radiation absorbed by the ground increases its temperature, causing a convection heat transfer between the ground and the air under the cover. Buoyancy drives the hot air near the ground to the cover. Suction from the chimney cause an updraft of the hot air, and ambient temperature air inlets on the periphery of the cover, generating a continuous airflow in the solar chimney. The airflow energy can be converted into mechanical energy by pressure staged wind turbines located at the base of the chimney and into electrical energy in conventional generators (Dai et. al., 2003).

The first experimental plant was built in 1981, in Manzanares, Spain. This solar chimney was 195 m high and covered an area of approximately 45.000 $m^2$, generating 50 kW of electrical power (Schlaich, 1995). There is another solar chimney under construction in Australia, with a tower 1000 m high, developed to generate 200 MW. Since the efficiency of the conversion from solar to electrical energy is very low, large plants are necessary to generate energy with viable costs. The hot airflow generated in the solar chimney can be used to dry agricultural products in smaller plants (Ferreira, 2004; Maia, 2005).

The agricultural products have several ranges of temperature and mass flow that ensure the best drying conditions, improving the quality of the dried products. A model capable of predict the velocity and temperature fields of the airflow generated in a solar chimney could be an useful tool to help the project of solar dryers. The purpose of this paper is to present an analytical and numerical study of the unsteady turbulent airflow in a solar chimney. The

mathematical model developed and the numerical methodology adopted were validated against the comparison of the theoretical results with experimental data obtained in a prototype.

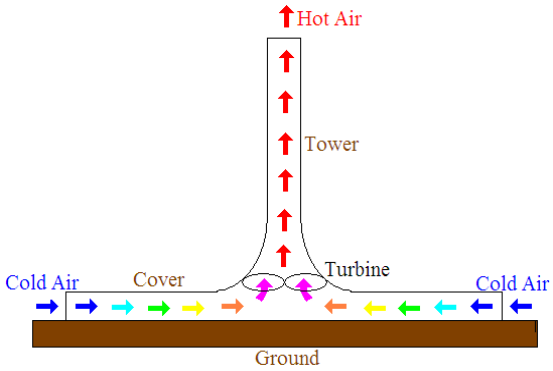


Figure 1 – Principle of the Solar Chimney

## 2. Theoretical model

It was developed a mathematical model for the airflow inside a solar chimney. The governing equations were numerically solved using the finite volume in generalized coordinates method. The analysis described in this paper is based on the following assumptions: the flow is axi-symmetric in the device, the heat losses through the tower are neglected, the airflow reaches turbulent intensities and air is considered a Newtonian fluid and an ideal gas.

The solution domain is showed in Fig. 2. The tower radius and height are, respectively, *Rt* and *Ht*. The cover radius is *Rc*. The cover height is *Hc2* at the entrance of the cover and it increases until *Hc1*, the maximum height.

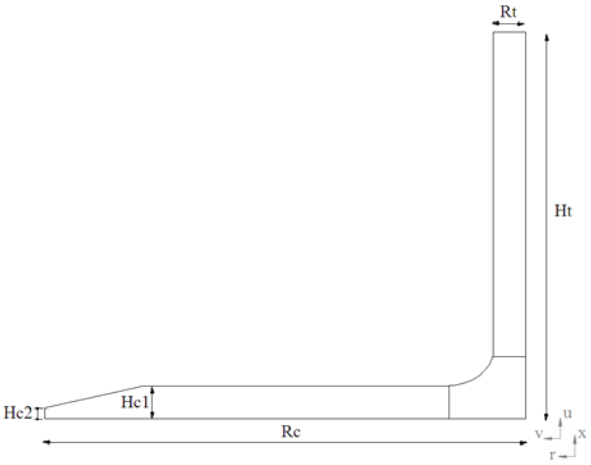


Figure 2 – Solution Domain

### 2.1. Governing equations

Assuming that the airflow is turbulent in the solar chimney, the governing equations are given in cylindrical coordinates (*r*, *x*) as:

Mass conservation

$$\frac{\partial \rho}{\partial t}+\frac{\partial}{\partial x}(\rho u)+\frac{1}{r}\frac{\partial}{\partial r}(r\rho v)=0 \tag{1}$$

x-momentum conservation

$$\frac{\partial}{\partial t}(\rho u)+\frac{\partial}{\partial x}(\rho uu)+\frac{1}{r}\frac{\partial}{\partial r}(r\rho uv)=-\frac{\partial}{\partial x}\left(p+\frac{2}{3}\rho k\right)+\frac{\partial}{\partial x}\left(\mu_e\frac{\partial u}{\partial x}\right)+\frac{1}{r}\frac{\partial}{\partial r}\left(r\mu_e\frac{\partial u}{\partial r}\right)+$$
$$\frac{\partial}{\partial x}\left(\mu_e\frac{\partial u}{\partial x}\right)+\frac{1}{r}\frac{\partial}{\partial r}\left(r\mu_e\frac{\partial v}{\partial x}\right)+(\rho_o-\rho)g \tag{2}$$

r-momentum conservation

$$\frac{\partial}{\partial t}(\rho v)+\frac{\partial}{\partial x}(\rho uv)+\frac{1}{r}\frac{\partial}{\partial r}(r\rho vv)=-\frac{\partial}{\partial r}\left(p+\frac{2}{3}\rho k\right)+\frac{\partial}{\partial x}\left(\mu_e\frac{\partial v}{\partial x}\right)+\frac{1}{r}\frac{\partial}{\partial r}\left(r\mu_e\frac{\partial v}{\partial r}\right)+$$
$$\frac{\partial}{\partial x}\left(\mu_e\frac{\partial u}{\partial r}\right)+\frac{1}{r}\frac{\partial}{\partial r}\left(r\mu_e\frac{\partial v}{\partial r}\right)-2\mu_e\frac{v}{r^2} \quad (3)$$

Thermal energy conservation

$$\frac{\partial}{\partial t}(\rho T)+\frac{\partial}{\partial x}(\rho uT)+\frac{1}{r}\frac{\partial}{\partial r}(r\rho vT)=\frac{\partial}{\partial x}\left[\left(\frac{\mu}{\mathrm{Pr}}+\frac{\mu_t}{\mathrm{Pr}_t}\right)\frac{\partial T}{\partial x}\right]+\frac{1}{r}\frac{\partial}{\partial r}\left[r\left(\frac{\mu}{\mathrm{Pr}}+\frac{\mu_t}{\mathrm{Pr}_t}\right)\frac{\partial T}{\partial r}\right]+$$
$$\frac{\beta T}{c_p}\left[\frac{\partial p}{\partial t}+\frac{\partial}{\partial x}(pu)+\frac{1}{r}\frac{\partial}{\partial r}(rpv)-p\frac{\partial u}{\partial x}-\frac{p}{r}\frac{\partial}{\partial r}(rv)\right] \quad (4)$$

In the above equations, $\rho$, $c_p$, $\beta$ and $Pr$ are the air density, specific heat, volumetric expansion coefficient and Prandtl number. $Pr_t$ is the turbulent Prandtl number and $\rho_o$ is the reference density of the air. $t$ represents the time, $u$ and $v$ corresponds to the axial and radial velocities, $p$ and $T$ represent the air pressure and temperature, respectively. $g$ corresponds to the gravity acceleration. $\mu_e$ is the effective viscosity, given as

$$\mu_e = \mu + \mu_t \quad (5)$$

where $\mu_t$ is the eddy viscosity of the flow and $\mu$ is the viscosity of the air.

The Launder and Spalding k-ε turbulence model (1974) with wall functions was used to evaluate the eddy viscosity. This model calculates the eddy viscosity in terms of the turbulent kinetic energy $k$ and its rate of dissipation $\varepsilon$ as

$$\mu_t = \rho C_\mu C_D \frac{k^2}{\varepsilon} \quad (6)$$

The turbulent kinetic energy and its rate of dissipation are evaluated through the transport equations given below.

Turbulent kinetic energy transport equation

$$\frac{\partial}{\partial t}(\rho k)+\frac{\partial}{\partial x}(\rho uk)+\frac{1}{r}\frac{\partial}{\partial r}(r\rho vk)=\frac{\partial}{\partial x}\left(\frac{\mu_e}{\sigma_k}\frac{\partial k}{\partial x}\right)+\frac{1}{r}\frac{\partial}{\partial r}\left(r\frac{\mu_e}{\sigma_k}\frac{\partial k}{\partial r}\right)+P_k+G_k-\rho C_d\varepsilon \quad (7)$$

Rate of dissipation of the turbulent kinetic energy transport equation

$$\frac{\partial}{\partial t}(\rho\varepsilon)+\frac{\partial}{\partial x}(\rho u\varepsilon)+\frac{1}{r}\frac{\partial}{\partial r}(r\rho v\varepsilon)=\frac{\partial}{\partial x}\left(\frac{\mu_e}{\sigma_\varepsilon}\frac{\partial\varepsilon}{\partial x}\right)+\frac{1}{r}\frac{\partial}{\partial r}\left(r\frac{\mu_e}{\sigma_\varepsilon}\frac{\partial\varepsilon}{\partial r}\right)+\frac{C_1\varepsilon}{k}(P_k+G_k)(1+0{,}8R_f)-C_2\rho\frac{\varepsilon^2}{k} \quad (8)$$

where $C_\mu$, $C_D$, $C_1$, $C_2$, $\sigma_k$ and $\sigma_\varepsilon$ are the model constants and $P_k$ is the production of the turbulent kinetic energy, given as

$$P_k=\mu_t\left[\left(\frac{\partial u}{\partial r}+\frac{\partial v}{\partial x}\right)^2+2\left(\frac{\partial u}{\partial x}\right)^2+2\left(\frac{\partial v}{\partial r}\right)^2+2\left(\frac{v}{r}\right)^2\right] \quad (9)$$

Due to its robustness, economy and acceptable results for a considerable amount of flows, the k-ε model has been the most used model for numerical predictions of industrial flows (Deschamps, 1998). However, it has deficiencies in situations involving buoyancy forces. This problem was treated by adding some terms on the turbulent transport equations, suggested by Rodi (1993).

$G_k$ is the turbulent kinetic energy production due to buoyancy effects,

$$G_k=-\frac{\beta g}{\rho}\frac{\mu_t}{\mathrm{Pr}_t}\frac{\partial T}{\partial x} \quad (10)$$

$R_f$ is the Richardson number, given as the ratio between the turbulent kinetic energy production due to buoyancy effects ($G_k$) and the turbulent kinetic energy production ($P_k$).

The turbulent model constants are presented in Tab. 1.

Table 1 – k-ε Model Constants

| $C_\mu$ | $C_D$ | $C_1$ | $C_2$ | $\sigma_k$ | $\sigma_\varepsilon$ |
|---|---|---|---|---|---|
| 0,09 | 1,0 | 1,44 | 1,92 | 1,0 | 1,3 |

**2.2. Boundary conditions**

The boundary conditions are shown in Fig. 3.

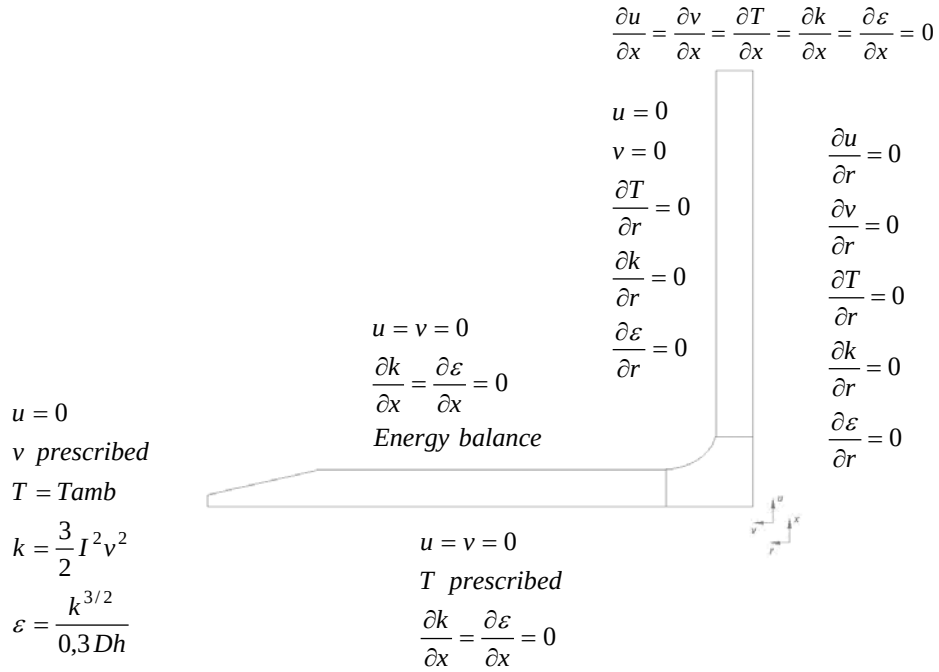


Figure 3 – Boundary conditions

The air temperature at the inlet of the cover is the ambient temperature. The *u*-velocity is assumed null and the *v*-velocity is evaluated through a mass conservation balance. The turbulent parameters are specified in terms of a turbulent intensity *I*, according to AEA (2001). The flow is assumed fully developed on the top of the tower and axi-symmetric on the center of the device.

The tower walls, the ground, the cover and the junction between the cover and the tower are wall regions. On the walls, non-slip conditions were adopted. The turbulence model assumes that the gradient of the turbulent parameters on the direction perpendicular to the main flow is null on walls. The flow is assumed thermal insulated on the chimney walls and on the junction between the cover and the tower. An energy balance is developed to the cover and to the ground.

The cover temperature is determined by an energy balance between the airflow in the solar chimney and the surroundings. The thermal energy lost from the cover to the surroundings by convection and infrared radiation equals the energy transferred by convection between the airflow and the cover and the thermal radiation exchanged between the ground and the cover.

The ground surface temperature is described by the energy conservation equation, with the simplifying assumptions of unsteady one-dimensional conduction through the ground and semi-infinite solid. The solar radiation absorbed by the ground and transmitted to the deeper layers is given as the difference between the incident solar radiation and the heat flux transmitted to the airflow by convection and to the cover by radiation.

**3. Validation of the mathematical model**

A prototype of the solar chimney was built in order to obtain experimental data to validate the mathematical model developed and the numerical methodology adopted. The tower of the prototype *Ht* was 12,3 m high and has a radius *Rt*

of 1 m. The radius of the cover *Rc* was 25 m and his height at the inlet *Hc2* was 0,05 m, increasing linearly up to *Hc1* = 0,5 m, in a radius of 20 m (Fig.2).

The computational code was simulated to the physical conditions observed on the prototype. Figure 4 shows the numerical and experimental temperatures on the ground surface. An agreement within 1,4°C was obtained with the present theoretical model.

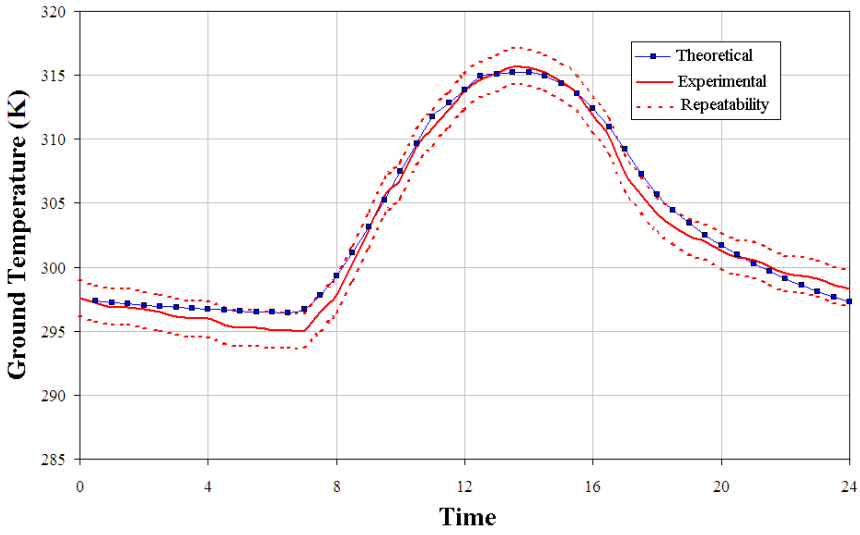


Figure 4 – Ground temperature during the day

The velocity of the airflow in the tower is shown in Fig. 5. It can be observed an increase on the velocity at around 4:30 a.m., not observed in the experimental results. This increasing can be explained by differences between the numerical and the real heat fluxes. Although the numerical data are out of the dispersion limits, the absolute difference between numerical and experimental values is lower than 0,3 m/s, but the relative difference is almost 25%. During the calibration of the anemometers, some problems were noticed, especially on lower velocities. Repeatability

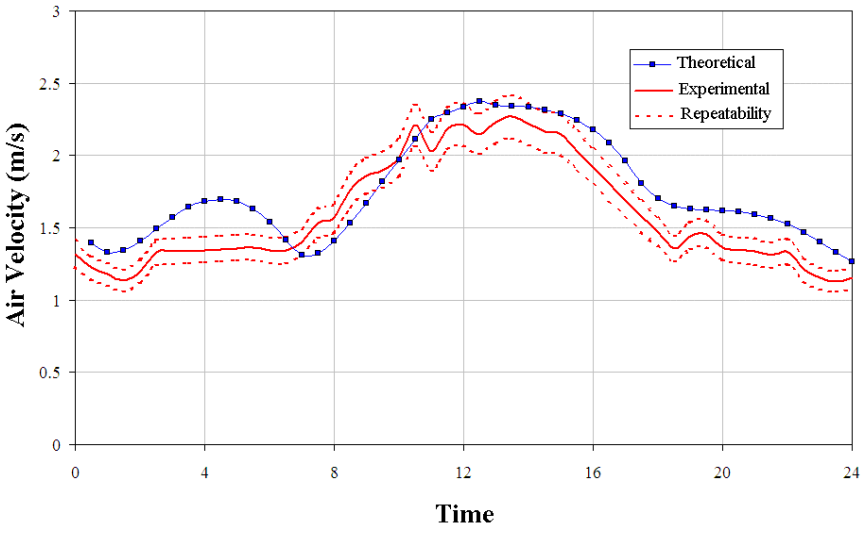


Figure 5 – Air velocity in the tower during the day

## 4. Results and discussions

The simulation of the airflow in the solar chimney was carried out with 376 control volumes on the direction of the main flow and 32 control volumes on the normal direction. The time increment was 5 minutes. The results presented were obtained to a solar chimney with the dimensions of the prototype.

The cover height at the periphery is 0,05 m, increasing to 0,5 m on a radius of 20 m. Since the cross sectional area increases towards the center of the cover with the height, the airflow velocity decreases. When the cover height reaches its maximum value, the velocity reaches its minimum value. The cross sectional area decreases towards the center of the

cover. Therefore, the velocity of the airflow increases up to the junction between the cover and the tower. This behavior can be seen in Fig. 6, which shows the development of the main velocity under the cover versus the dimensionless radius of the cover. The inlet of the cover corresponds to r/Rc = 1 and the center of the cover corresponds to r/Rc = 0.

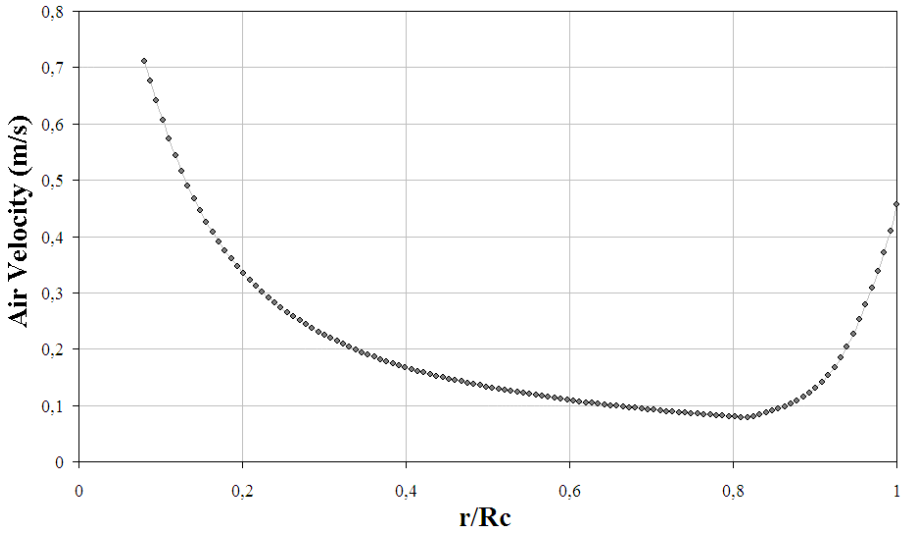


Figure 6 – Air velocity under the cover as function of the dimensionless cover radius

The velocities reached by the airflow are such that the flow in the solar chimney is turbulent. The profile of the velocity is characteristic of the turbulent flows. In the tower, the airflow velocity does not have significant modifications.

Figure 7 shows the airflow temperature under the cover as function of the dimensionless cover radius, in three heights. At the inlet of the cover, the temperature is the same, the ambient temperature. The air is heated by the ground, causing a reduction of the temperature from the ground to the surface of the cover. The same behavior is observed to all the heights evaluated. The largest gradients of temperature are found in the area near to the entrance, due to the largest differences between the ground and the inlet air temperatures. The temperatures increase towards to the center and, at some point, there are only observed slight modifications. On the junction region, it is observed an increasing of the temperature, explained by the thermal insulation condition imposed. Due to this boundary condition, the temperature in the tower does not show significant variations.

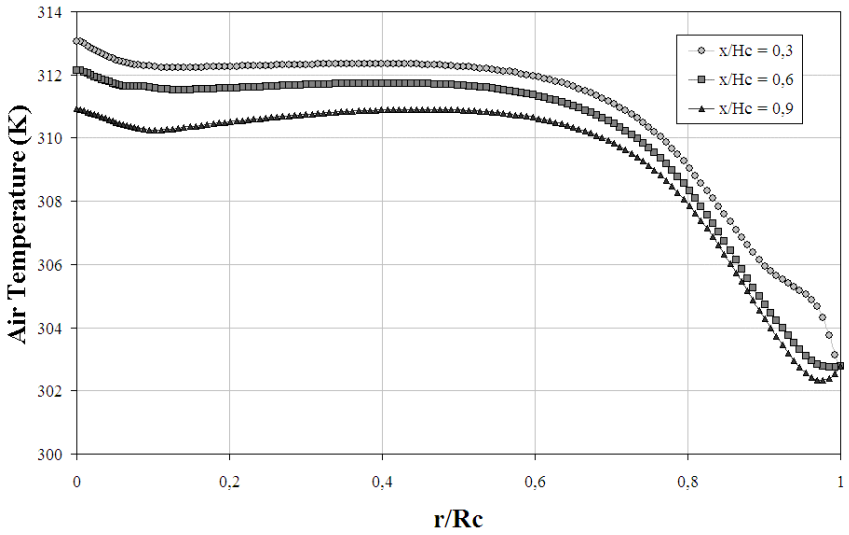


Figure 7 – Air temperature under the cover as function of the dimensionless cover radius, to different dimensionless cover heights

The behavior described before is valid to a solar chimney with the dimensions of the prototype. If some geometrical parameters were changed, some differences may occur. Figure 8 presents the development of the velocity under the cover, to a height corresponding to x/Hc = 0,5, evaluated to four different values of the radius cover. The higher the

radius cover, the higher the contact area between the airflow and the heated ground. For lower radiuses, the air temperature increases towards the center of the solar chimney. For larger radiuses, the air temperature only increases until a limit position is reached.

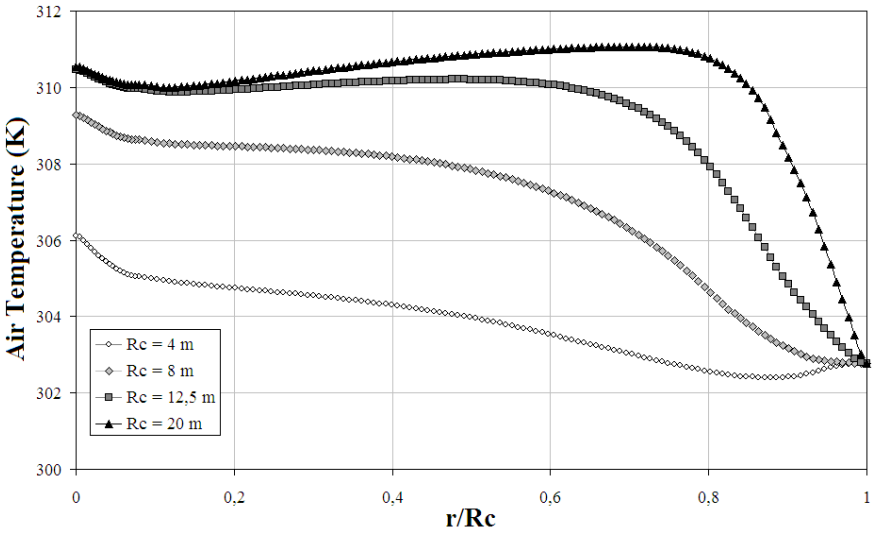


Figure 8 – Air temperature under the cover as function of the dimensionless cover radius, to different cover radius

The k-ε turbulence model of Launder and Spalding (1974) with function walls was used to obtain the results showed above. The flow was also simulated with RNG k-ε model proposed by the Renormalization Group (Yakhot e Orszag, 1982). Figure 9 shows the air velocity at the center of the tower to the turbulence models evaluated, along with the experimental data. The numerical results are very close to both models, being slightly lower to RNG k-ε model. Great differences can be observed comparing the numerical and the experimental data, as discussed before. The maximum difference is about 25% for the Launder and Spalding k-ε model and about 26% for RNG k-ε model.

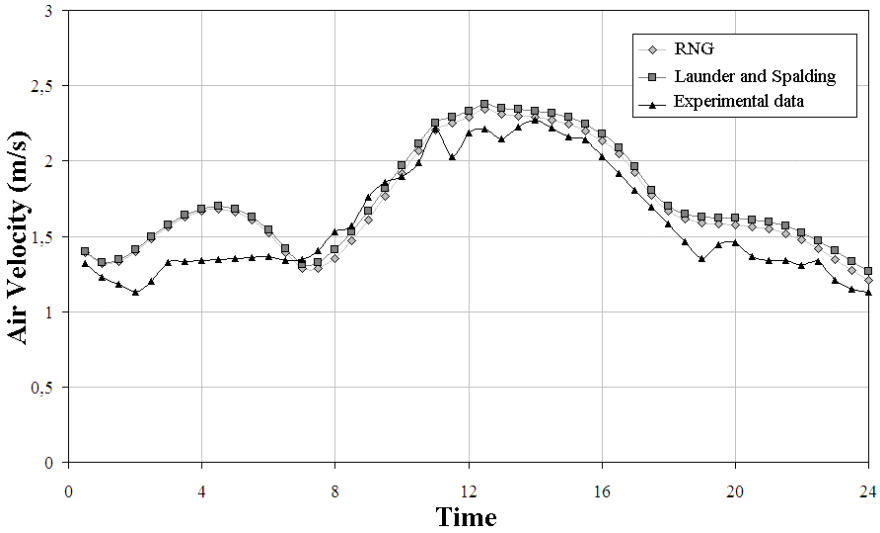


Figure 9 – Comparison of the air velocity in the tower to the turbulence models and to experimental data

Figure 10 shows the development of the air temperature under the cover, on a height corresponding to x/Hc = 0,5. The RNG k-ε model has lower temperatures than Launder and Spalding k-ε model, but the differences between the models are negligible. The maximum difference between experimental data and Launder and Spalding k-ε model was about 1% and between experimental data and RNG k-ε model, 2%.

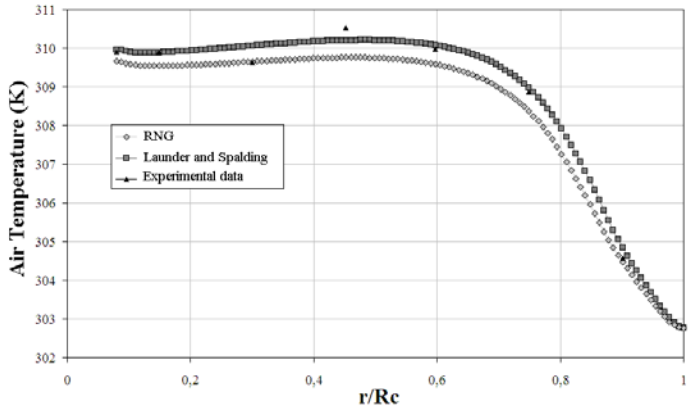


Figure 10 – Comparison of the air temperature under the cover to the turbulence models and to experimental data

## 5. Conclusions

This paper presented an unsteady analysis of the turbulent airflow in a solar chimney. The proposed mathematical model includes the conservation laws for mass, momentum and thermal energy and the transport equations for the turbulence model variables. A computational code using the Finite Volume Method in Generalized Coordinates was adopted to solve the system of equations which describe the flow. The validation of the proposed mathematical model and numerical methodology was done through comparison of the theoretical results and the experimental data obtained in a prototype. A good agreement was found between the theoretical and the experimental results. The numerical results are capable of represent the airflow in a solar chimney.

The mathematical model developed was used to predict the behavior of the airflow in the solar chimney. Two turbulence models were evaluated, Launder and Spalding k-ε model with wall functions and RNG k-ε model. The differences between both models were insignificant.

The development of a mathematical model is a powerful tool to help on the project of solar chimneys and on the analysis of its technical and economical viability. The airflow temperatures and velocities can be predicted to several geometrical configurations, materials and structures. Therefore, geometrical and operational parameters can be determined for the optimum operation of solar chimneys to generate electrical energy or to dry agricultural products.

## 6. References

AEA Technology Engineering Software Limited, 2001, CFX – TASCFlow User Documentation, Version 5.5, Waterloo, Canada.

Deschamps, C.J., 1998, “Modelling of turbulent flow through radial diffuser”, Anais da I Escola de primavera de Transição e Turbulência, Vol I, pp 21-43.

Dai, Y.J., Huang, H.B., Wang, R.Z., 2003, ”Case study of solar chimneys power plants in northwestern regions of China”, Technical note, Renewable Energy, Vol. 28, pp 1295-1304.

Ferreira, A. G., 2004, “Avaliação da Viabilidade Técnica de Chaminés Solares para a Secagem de Alimentos”, Tese de Doutorado, Universidade Federal de Minas Gerais, Belo Horizonte.

Launder, B.E. e Spalding, D.B., 1974, “The Numerical Computation of Turbulent Flows”, Computer Methods in Applied Mechanics, Vol. 3, pp 269-289.

Maia, C.B., 2005, “Análise Teórica e Experimental de uma Chaminé Solar: Avaliação Termofluidodinâmica”, Tese de Doutorado, Universidade Federal de Minas Gerais, Belo Horizonte.

Rodi, W., 1993, “Turbulence Models and their Application in Hydraulics – A State of Art Review”, IAHR, 3rd Edition, Rotterdam, A.A. Balkema.

Schlaich, J., 1995, “The Solar Chimney, Electricity from the Sun”, Edition Axel Menges, Stuttgart, 59p..

Yakhot, V. e Orszag, S.A., 1992, “The Renormalization Group: The Eps Expansion and Derivation of Turbulence Models”, Journal of Scientific Computing, Vol. 7, No. 1, pp 35-61.

## 7. Responsibility notice

The authors are the only responsible for the printed material included in this paper.

## 8. Thanks

This job was realized with the support of the Fundação de Amparo à Pesquisa do Estado de Minas Gerais - FAPEMIG and Conselho Nacional de Desenvolvimento Cientifico e Tecnológico CNPq – Brazil.